RESPONSE OF GAS PAYLOAD (G 345 AND G 347) TEMPERATURES TO VARIOUS ORBITER FLIGHT ATTITUDES

Werner M. Neupert
Laboratory for Astronomy and Solar Physics
NASA/GSFC, Greenbelt, Maryland

Presented at Second GAS Experimenters Symposium
October 8, 1985

I. INTRODUCTION

At the beginning of the Get-Away Special (GAS) flight program, the GAS Project flew a Flight Verification Payload on STS-3 to make measurements of the vibrations, acoustic and magnetic environments of the canister, and to obtain thermal profiles of internal and external components of the GAS system. These data were used to verify pre-flight thermal models of the GAS system and results have been published in a GSFC Technical Note, X-732-83-8 (Butler, 1983). On somewhat later flights of the Orbiter, STS-7 and STS-8, the Naval Research Laboratory and the Goddard Space Flight Center jointly developed and flew a GAS payload whose primary objective was to evaluate the performance of ultraviolet-sensitive (Schumann) photographic emulsions in the Orbiter environment, including pre-flight integration, on- orbit exposure to the ambient environment of the Orbiter bay and post-flight conditions before removal of the experiment from the vehicle. These emulsions, used in spectrographs to record solar radiations with wavelengths between 100 A and 2000 A, have low gelatin content and no protective gelatin overcoating in order to maximize their UV sensitivity. Consequently, they are extremely sensitive to environmental conditions. Furthermore, they are exposed directly to space during the observations because any intervening protective window or lense would completely absorb the radiations to be studied. Our instrument, which was prepared at the Naval Research Laboratory under the direction of Robert Kreplin (Kreplin et al., 1984 a) also included two thermal sensors, whose output was recorded once an hour with a precision of 0.7° C. The experiment operated nominally on both missions and provided important data confirming that UV - sensitive emulsions could tolerate integration and flight on the Shuttle with relatively little deterioration. The results of these studies have already been reported (Kreplin et al, 1984 b). The temperature measurements also were recorded successfully and are the basis for this paper. They are a useful complement to the thermal observations made on STS-3 and provide additional insight into the reaction of a payload to typical thermal environments that GAS experiments are subject to.

Our GAS experiment and the circumstances of its flights were particularly useful in terms of modeling the thermal response of the GAS canister and our instrument. The Orbiter was held (except for interuptions for star tracker alignment, satellite deployments, etc., in specific attitudes for sufficiently long periods of time that the thermal response of the instrument to each attitude was well measured. Two types of GAS canister end cap, one, the insulated end cap and the other a silverized teflon covered end-cap, were used on the two flights so that a direct comparision of the thermal performance of the two types was obtained.

This report is an attempt to compare these observations with a simple thermal model of the instrument in the GAS canister in order to assess whether such simple models can be useful to experimenters in predicting the thermal response of their payloads.

II. Instrumentation and Observations

A crosssectional view of the instrument is shown in Figure 1. The EMP is at the top of the diagram. The experiment was directly mounted to it using two thick aluminum support rings. The major components of the experiment, in terms of thermal mass, were the doughnut - shaped battery container mounted directly to the support rings, the cylindrical Main Experiment Container, carrying the photographic emulsion samples, and also mounted directly to a support ring, and the cylindrical electronics box attached to the Main Experiment Container.

Temperatures were measured at two locations using thermistor networks (thermilinear component YSI No. 44203 incorporating a bead thermistor (YSI 44018)). These were supplied by the Yellow Springs Instrument Co. One sensor was located inside the Main Experiment container on the flange supporting the inner film cylinders. The second was located on one of the brackets supporting a film cylinder on the outside of the Main Experiment Container. The location of these two sensors, effectively at each end of the Main Experiment Container, provided a means of measuring temperatures and temperature gradients along the Main Experiment Container and inner film cylinders.

The data obtained for flights of this instrumentation on STS-7 and STS-8 are shown in Figures 2 and 3 (See also Kreplin et al, (1984). Data from the two sensors (shown by solid and dashed lines) are very nearly the same. The small differences are not consistent, and may be due to errors of roundoff in the digitization, etc. On each flight the experiment power was turned on internally using altitude switches (Altitude/ Absolute Pressure Switch E45C-72 (50,000 ft. turn-in) backed-up with E45C-73 (70,000 ft turn-on). These switches were obtained from Precision Sensors, Inc.

The first flight of our instrument, designated G 345, began with an extended period of about 70 hours during which the Orbiter flew with its bay facing the earth (-Z Local Vertical, abbreviated to -Z LV). This orientation was held for 70-75% of the time, being interupted by scheduled satellite deployments, etc. In this attitude the payload cooled rapidly $-8.4^{0}C$, consistent with but slightly lower than the nominal - $5^{o}C$ equivalent sink temperature expected for this orbiter orientation. Following this period, the Orbiter attitude was changed so that the bay faced deep space (equivalent sink temperature of - $100^{o}C$), for about 2.5 hrs during deployment of the European SPAS subsatellite and the payload temperature dropped. A more substantial temperature drop was recorded between 92 and 100 hours Mission Elapsed Time (MET) when the Orbiter bay again faced deep space during the SPAS operations and retrieval. The payload temperature dropped for about 4 hours after the Orbiter returned to -Z Local Vertical attitude, then began to

increase again, approaching the steady-state temperature of -8.4C recorded earlier in this flight.

Eventually, at landing, the temperature rose, with no overshoot, and showed a daily variation about 5^0 before the temperature recording was terminated.

The flight of STS-8, carrying the same experiment but a different, insulating, GAS canister end-cap and designated G 347, also began with an extended period of 34 hrs. of -Z Local Vertical orientation. The payload temperature dropped much more slowly than for G-345, although the flight began with the same Orbiter attitude. This was the result of adding the insulating end cap. After 34 hours MET the Orbiter was re-oriented to a tail to sun attitude during which the bay of the Orbiter always faced away from the earth, i.e. into deep space. This attitude is called - X Solar Inertial, Orb Rate, abbreviated to - X SI, Orb Rate, as the Orbiter rotates once an orbit about its longitudinal (X) axis. Neither direct nor earth-reflected sunlight illumined the Orbiter bay during this attitude for which the sink temperature again was - 100°C. The payload temperature dropped rapidly, continuing to do so for about 20 hours after the - Z Local Vertical attitude was re-established at 48 hours MET. The remainder of the flight was spent for the most part at - Z and + X Local Vertical (Orbiter nose (+X) or tail(-X) pointing toward the earth) and the payload equilibrated at about - 5 °C, the nominal sink temperature for the - Z Local Vertical attitude.

III. Thermal Modeling of the Payload

Thermal modeling of the payload, for purpose of obtaining a comparison with the in-orbit temperature measurements, began by adopting a simplified thermal model, shown in Figure 4. The major structural components of the instrument were identified as:

1. The battery pack baseplate of T6061 aluminum, and attached to the GAS Experiment Mounting Plate (EMP) via two heavy aluminum (T6061) spacer rings.

2. The battery pack itself, the housing of aluminum and carrying 34 alkaline "D" cells held in a fixed assembly by machined teflon rings.

3. The Main Experiment Container, including all inner and outer film cylinders, all control valves, etc., made primarily of stainless steel.

4. The electronics box, the housing of which was made of T6061 aluminum, together with an electronics module containing components, mounting boards, etc. For purpose of the model, the electronics box was assumed to be 50% aluminum and 50% fiberglass.

All aluminum experiment surfaces were iridited (for which we assumed an emittance of 0.09, the mean of values given by Butler) and the stainless steel was passivated. An emittance of 0.17 , typical for mechanically polished stainless steel, was used (Wolfe, 1965).

As an initial step, in an attempt to simplify further calculations, the heat loss of the individual major components was estimated using standard equations for conductive and radiative transfer given by Butler (Figure 5). Modeling of the thermal response of the instrument was simplified because internal power dissipation was extremely low (12 - 13 milliwatts) and could be neglected, and internal convection was not present, as the experiment was exposed to the vacuum of space through a purge port in the Experiment Mounting Plate (EMP). Radiative view factors for infinite concentric cylinders were used as being most appropriate for this experiment . For this geometry the effective emmittance is given by:

$$\varepsilon_{1,eff} = \varepsilon_1 F_{2-1} = \frac{1}{\frac{1}{\varepsilon_1} + \frac{A_1}{A_2}\left(\frac{1}{\varepsilon_2} - 1\right)}$$

where A, and A_2 are the areas of the two concentric surfaces and ε_1 and ε_2 are their emittances. (Wolfe, 1965). The estimated heat loss and consequent temperature drop per hour for two typical temperature differentials is shown in Figure 6. The very good conductive coupling between the GAS EMP and the base of the battery pack baseplate via the very heavy aluminum spacer rings means that the baseplate temperature will very closely track the EMP temperature. For subsequent calculations we therefore assumed that this baseplate was effectively a portion of the GAS canister and increased its effective mass accordingly. Likewise, the battery pack temperature itself will also track the EMP temperature quite well and can be assumed to be thermally a part of the EMP.

The remaining components of the experiment were less well thermally coupled to the EMP and it became clear from the model that both conductive and radiative losses to the GAS canister had to be considered, Radiative losses by the electronics box were particularly important for cooling that module. Conductive coupling to the EMP was low because of the low conductance of the thin walled stainless steel Main Experiment Container. The conductive losses given in Figure 6 are an upper limit as the contact resistance of the various mechanical joints has not been included - Note that the temperature drops in the Main Experiment container and electronic box are predicted to be within a degree of one another as is confirmed by actual temperature readings of the two probes, so that net heat transport between the Main Experiment Container and electronics box could be considered to be negligible.

Using these preliminary results, we simplified our thermal model, i.e the battery pack and its baseplate became a part of the GAS canister and the thermal contribution of the electronics box to the temperature of the Main Experiment Container was assumed to be negligible. Hence, a final thermal model of the Main Experiment Container included only radiative and conductive interaction with the GAS canister.

IV. Results

This simple model of the experiment was set up on a desk calculator using external boundary conditions for the flight of G 347 (Figure 7). A sink temperature of -5°C (268K) was used for the -Z LV attitude and -100°C (173K) during - X SI with bay facing away from the earth. Temperatures were calculated at hourly intervals and sink temperatures changed in accordance with the as-flown flight plan (short intervals of orbiter maneuvering being disregarded). Criteria used to evaluate the accuracy of the model were agreements between calculated and observed temperatures at the end of the -Z LV interval at 34 hr MET, at the end of the -X SI interval at 48 hr MET, and the timing and value of the minimum temperature after return to the -Z LV attitude.

Using nominal thermal properties of the experiment materials the calculated temperature profile for the G 347 flight (Figure 8) was substantially below the measured values. It appears, from Figure 8, that the Main Experiment Container is not as tightly coupled to the GAS canister as we had calculated. If we decouple it (reduce both radiative and conductive losses to the canister by a factor of 3.3) we can then match the observed temperatures at the end of -Z LV and -X SI, Orb Rate, but not the timing of the temperature minimum, which now occurs later in time because of the increased thermal isolation of the experiment. This case is shown in Figure 9.

We can now use this thermal model, with reduced experiment conductance and emittance to the GAS canister, to predict the thermal behavior of the experiment during the STS-7 flight. The results are shown in Figure 10. The calculated temperatures are appreciably higher than observed values. Two cases are shown in Figure 10. Case A was obtained using a nominal sink temperature of -5°C. A more appropriate sink temperature appears to be -8.4°C, the value used in calculating case B. In either case, the experiment temperature does not decrease rapidly enough because of the decoupling of the experiment from the GAS canister assumed (in Figure 9) to force a match to G 347 temperatures.

We can explore the possibilities of altering the emittance of the GAS canister as a way of improving the agreement between model and observations. One such combination of reduced experiment emittance and conductance reduced by a factor of 2.5) together with slightly reduced canister emittance (from 0.065 to 0.055) is shown in Figure 11. The agreement with experimental data is not appreciably better than for our earlier case (Figure 9). However, if this second model is used for the G 345 flight, the results, in Figure 12, are appreciably closer to the observations than the earlier calculations were.

There may be several other reasons for the discrepancy between G 345 data and predictions. For one, the Orbiter was flown in the thermally benign -Z Local Vertical attitude only about 70-75% of the tracker/navigational base re-calibrations, etc., could have been at less benign, i.e., colder thermal orientations, producing a faster than expected temperature drop on average. Yet another reason might be the crudity of the thermal model that we have used here.

In conclusion, the procedures outlined in the GAS Thermal Design Summary appear to give valid results when applied to an actual flight experience. They will provide useful predictions and should be used by any GAS experiments with a critical thermal requirement for his or her payload. In addition, we found some evidence that the average canister emittances may be slightly different from values given in the GAS Thermal Design Summary, but more data must be taken and evaluated before this can be established with certainty.

REFERENCES

1. Butler, D., 1983, "Get Away Special (GAS) Thermal Design Summary, GSFC Technical Note X-732-83-8.

2. Dohne, B., Feldman, U. and Neupert, W., 1984, "Aging Properties of Kodak Type 101 Emulsions", Appl. Opt. 23, 589.

3. Hall, D. F. and Fote, A. A.., 1981 "α_S/ϵ_H Measurements of Thermal Control Coatings on the P78-2 (SCATHA) Spacecraft," in "Heat Transfer and Thermal Control", Progress in Astronautics and Aeronautics, Vol. 78, pg 467.

4. Kreplin, R. W., Dohne, B., Feldman, U. and Neupert, W. M., 1984 "Effects of Shuttle Bay Environment on UV Sensitive Photographic Film, - Instrumentation for Get-Away-Special" Paper AIAA-84-0449, AIAA 22nd Aerospace Sciences Meeting, Reno, Nevada.

5. Kreplin, R. W., Dohne, B, Feldman, U. and Neupert, W. M., 1984 "Effects of Shuttle Bay Environment on UV Sensitive Photographic Film, - Results of Measurements Aboard STS-7 and STS-8" Paper AIAA-84-0293, ibid.

6. Wolfe, W. L., 1965, editor, "Handbook of Military Infrared Technology" Office of Naval Research, Department of the Navy, U.S. Government Printing Office.

ORIGINAL PAGE IS
OF POOR QUALITY

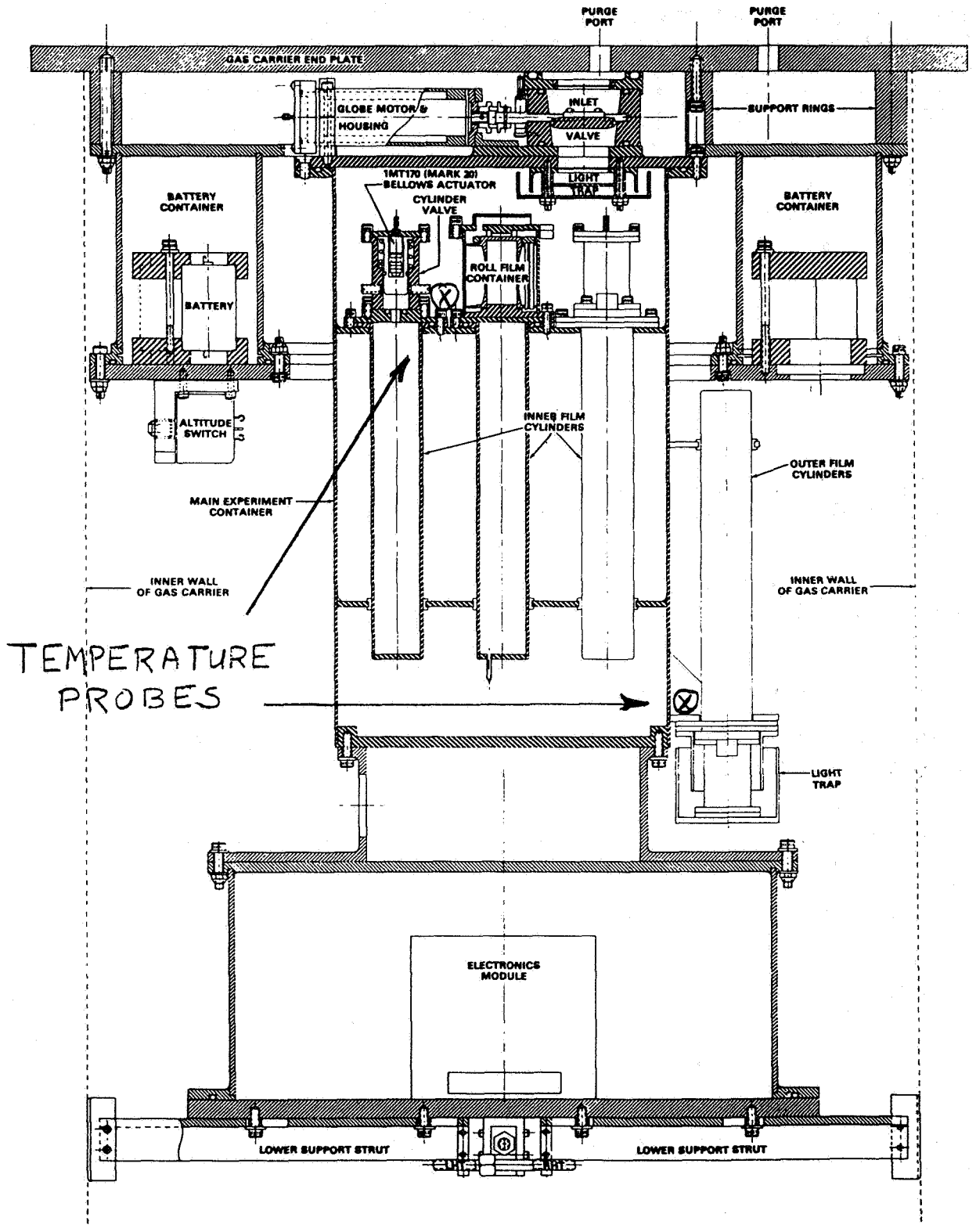

Figure 1. Cross-sectional view of the G.S.F.C./N.R.L. GAS Experiment for evaluating UV-sensitive photographic emulsions in the Orbiter environment.

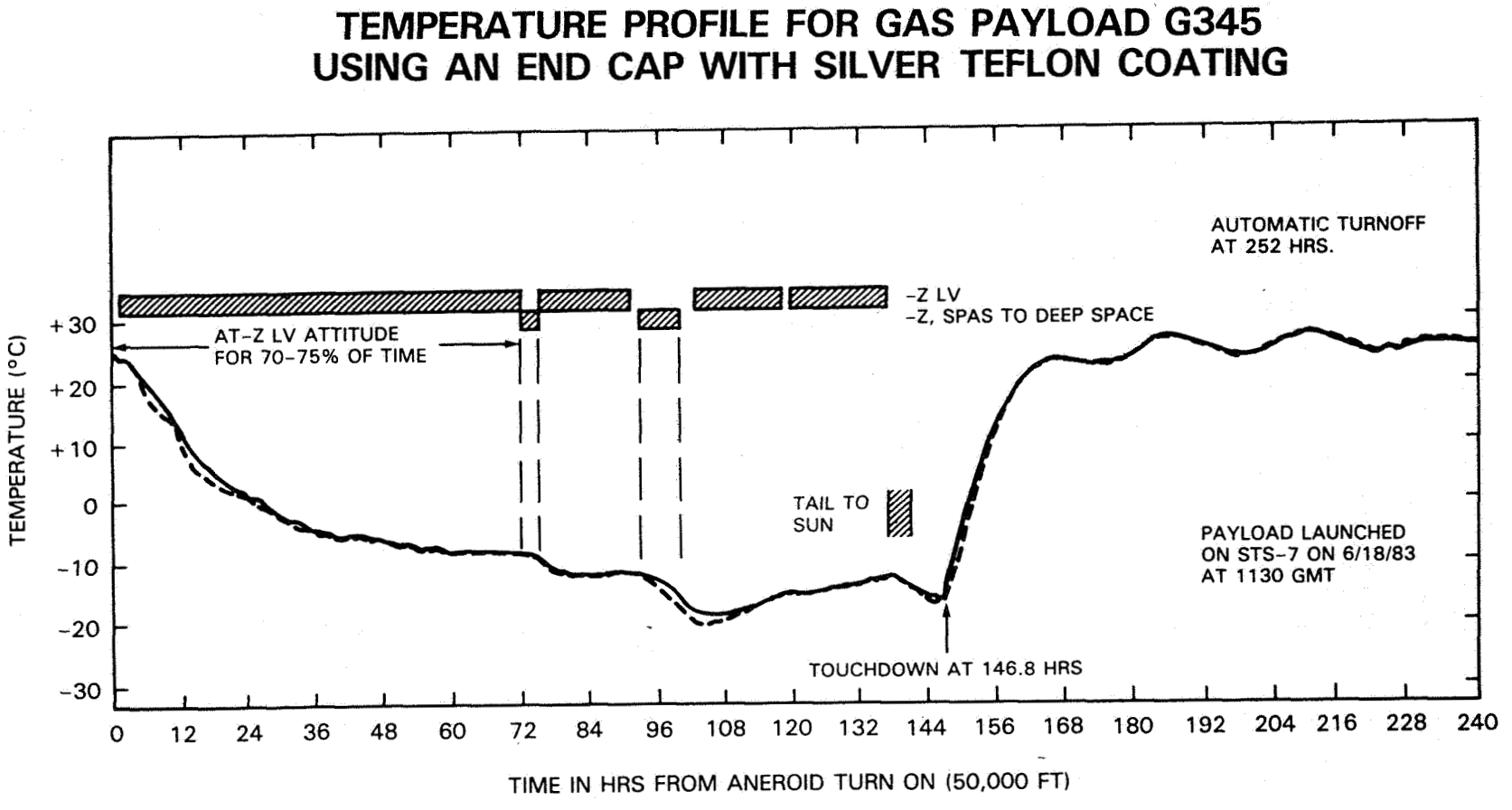

Figure 2. Experiment temperature data obtained from two sensors during the flight of GAS Payload G 345 on STS-7. Orbiter attitudes maintained during the flight are also shown.

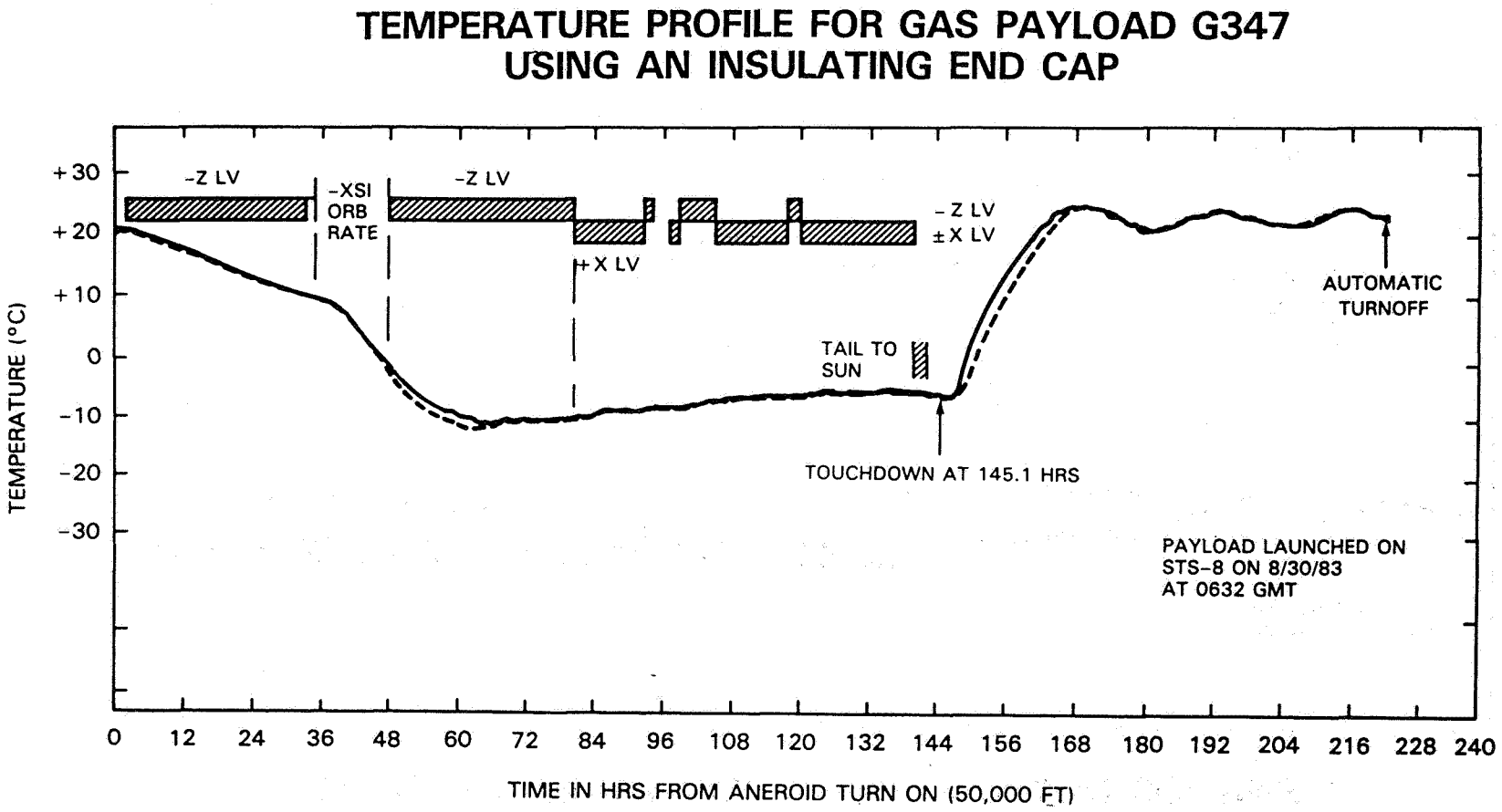

Figure 3. Experiment temperature data obtained from two sensors during the flight of GAS Payload G 347 on STS-8. Orbiter attitudes maintained during the flight are also shown.

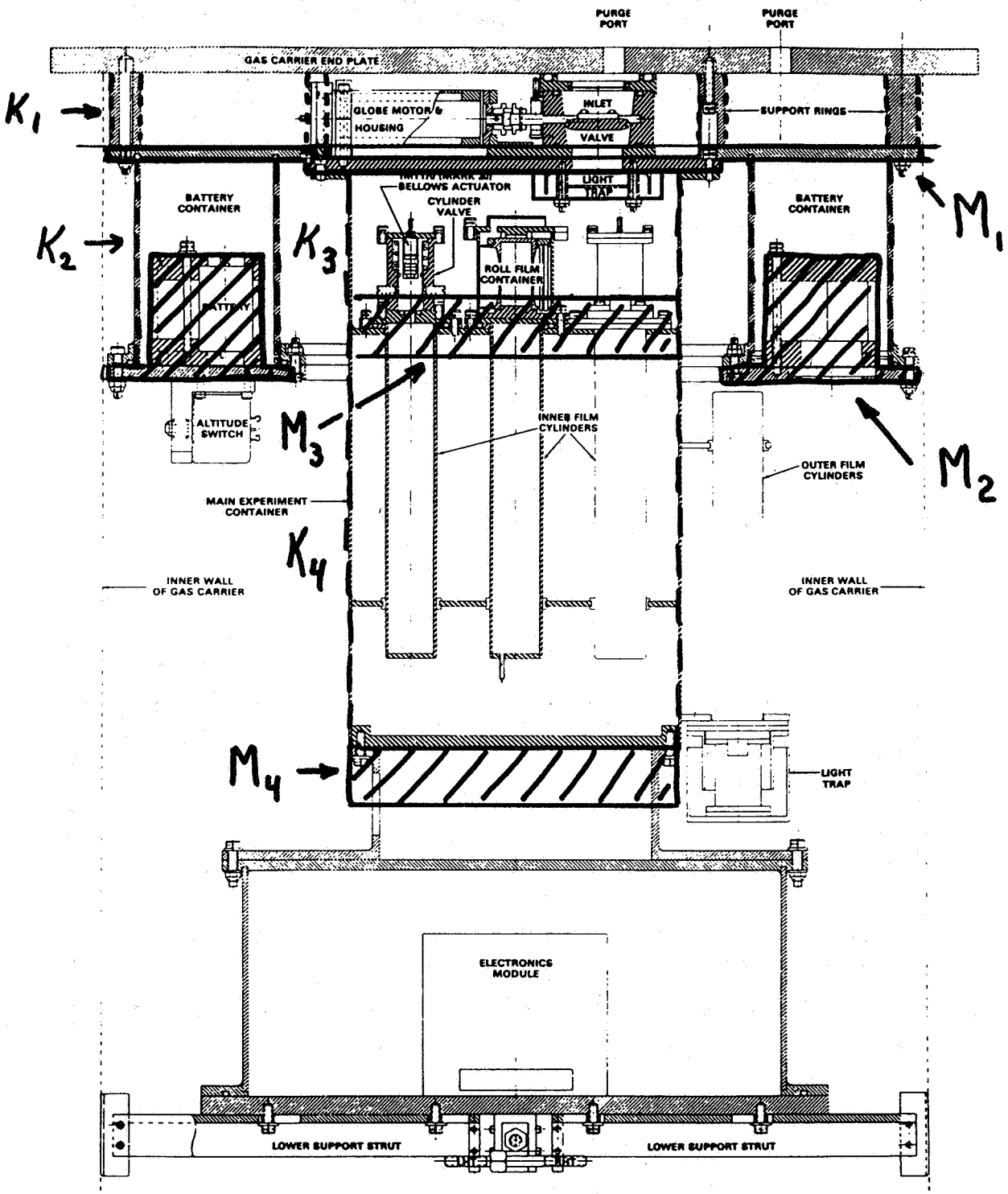

Figure 4. Simplified model of GAS experiment showing lumped subsystem masses used in our analysis.

$$Q_{LOST} = Q_{COND} + Q_{RAD} + Q_{CONV} = MC_p \Delta T$$

$$Q_{COND} = \frac{K_i A_i}{L_i} (T_i - T_{GAS}) \Delta t = K_i (T_i - T_{GAS}) \Delta t$$

$$Q_{RAD} = \sigma A_i \varepsilon_i F_{2-1} (T_i^4 - T_{GAS}^4) \Delta t$$

$$Q_{CONV} \equiv 0$$

K (Al) = 155.8 $W/_{m\,K}$

K (S.S.) = 16.3

ε (Al) = 0.09 (iridited)

ε (S.S.) = 0.17 (passivated)

C_p (Al) = 0.21 $cal/_{gm\,K}$

C_p (S.S.) = 0.11

Figure 5. Equations and data used in estimating thermal losses of experiment subsystems.

				$T_i - T_{GAS} = 5°$			$T_i - T_{GAS} = 10°$		
i	Subsystem	K_i	$(MC_p)_i$	Q_{COND}	Q_{RAD}	ΔT	Q_{COND}	Q_{RAD}	ΔT
1	Battery Pack Base plate	34.6	160	6.2×10^5	–	5°	12.4×10^5	–	10°
2	Battery Pack	0.74	2700	13,300	290	≈5°	26,600	600	≈10°
3	Main Experiment Container	0.042	1220	770	460	≈1°	1550	980	≈2°
4	Electronics	0.017	3500	290	360	≈0.2°	580	765	≈0.4°

UNITS

K : calories / K

M : grams

C_p : calories/gram K

Q : calories/hr

T : °C

Figure 6. Estimates of thermal losses and temperature changes of GAS Subsystems for two typical experiment/canister temperature differentials.

$$T_{GAS}(t+\Delta t) = T_{GAS}(t) - \frac{3600}{(MC_p)_{GAS}} \left\{ (6A\varepsilon_{eff})_{GAS} \left(T_{GAS}^4(t) - T_{ext}^4(t) \right) \right.$$

$$- \left(T_{EXP}(t) - T_{GAS}(t) \right) \left(K_3 + K_4 \right)$$

$$\left. - \left(T_{EXP}^4(t) - T_{GAS}^4(t) \right) \left((6A\varepsilon_{eff})_3 + (6A\varepsilon_{eff})_4 \right) \right\}$$

$$T_{EXP}(t+\Delta t) \equiv T_3(t+\Delta t) = T_{EXP}(t) - \frac{3600}{(MC_p)_3} \left[K_3 \left(T_{EXP} - T_{GAS} \right) \right.$$

$$\left. + (6A\varepsilon_{eff})_3 \left(T_{EXP}^4(t) - T_{GAS}^4(t) \right) \right]$$

where subscripts are defined in Fig. 6, and

$$T_{ext}(-Z\ LV) = 268\ K \ ; \ T_{ext}(-X\ SI) = 173\ K$$

Figure 7. Equations used in modeling thermal performance of Main Experiment Container and GAS canister for G 345 and G 347.

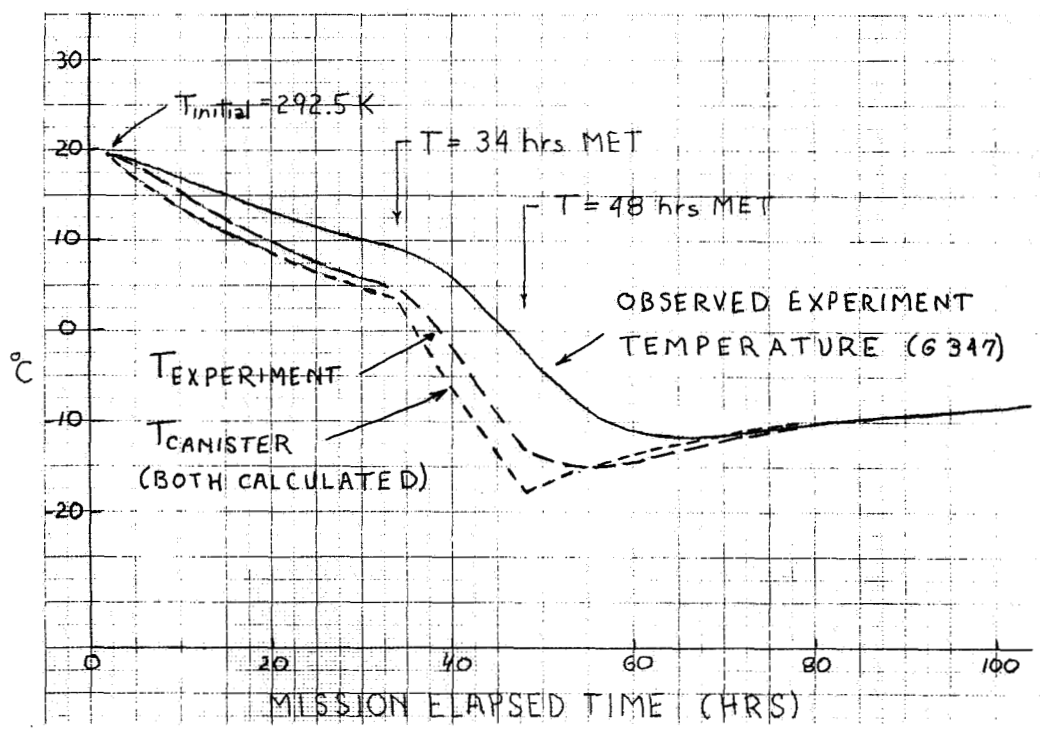

Figure 8. Comparison of calculated experiment and canister temperatures with observed G 347 experiment temperatures using nominal thermal properties for experiment and canister.

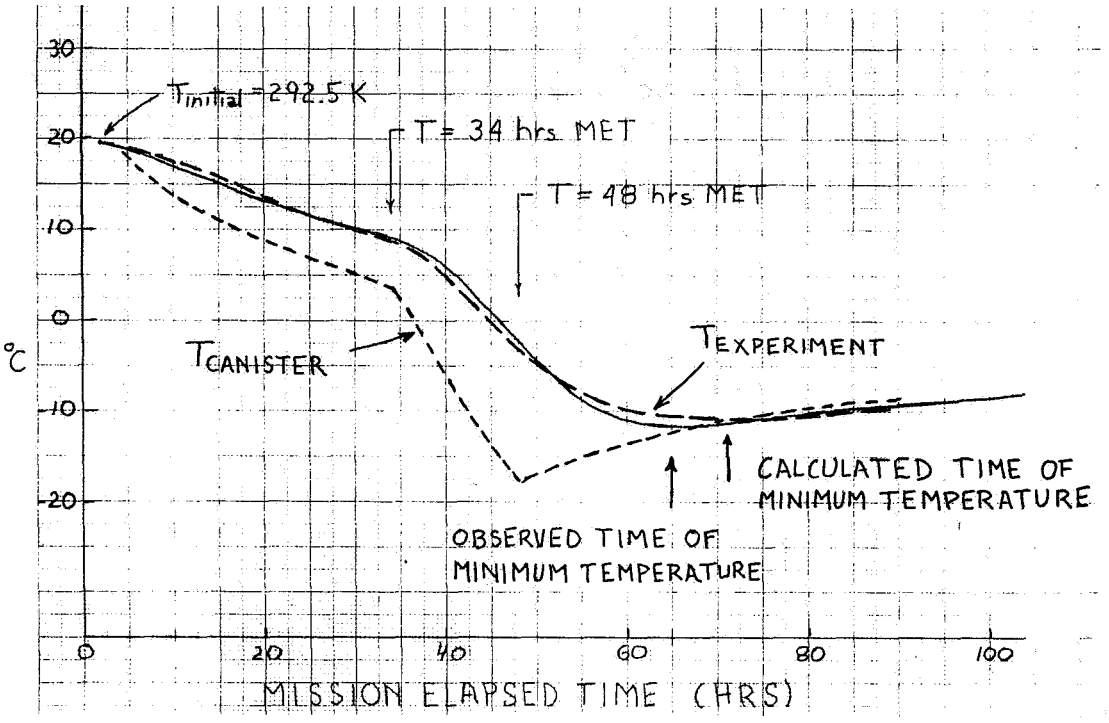

Figure 9. Comparison of G 347 calculated and observed temperatures using reduced experiment thermal conductance and emittance (0.3 of nominal values) but nominal canister emittance.

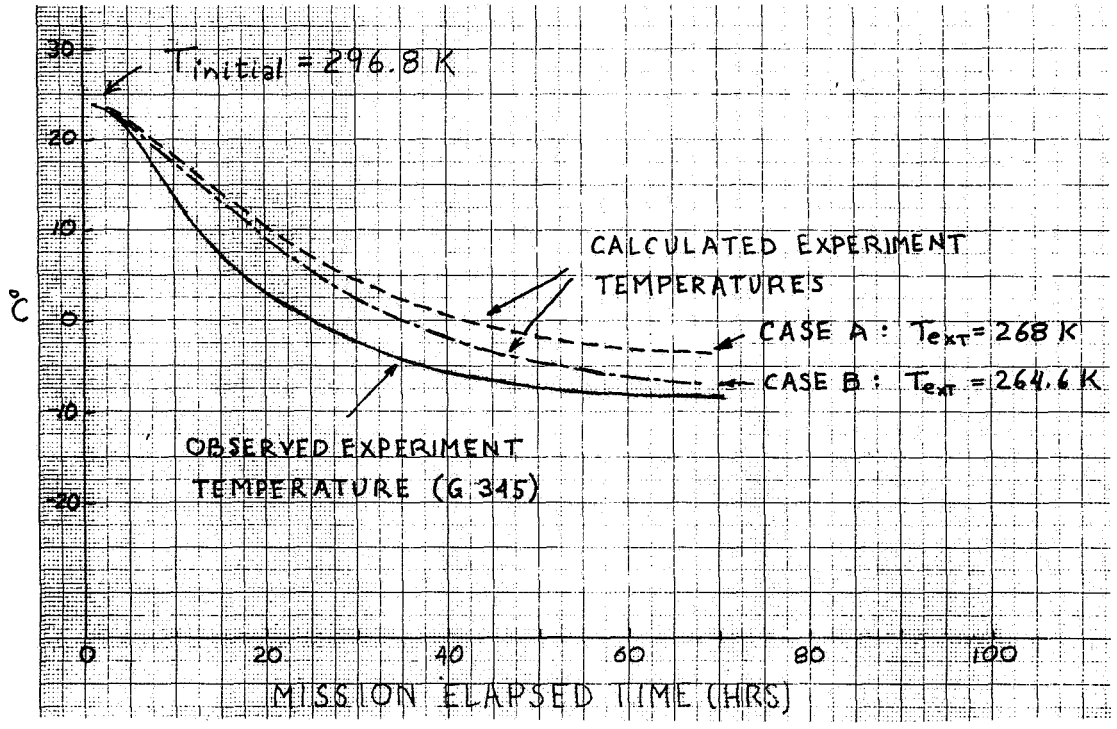

Figure 10. Comparison of G 345 calculated and observed temperatures using reduced thermal conductance and emittance (0.3 of nominal values) and nominal canister emittance (0.16).

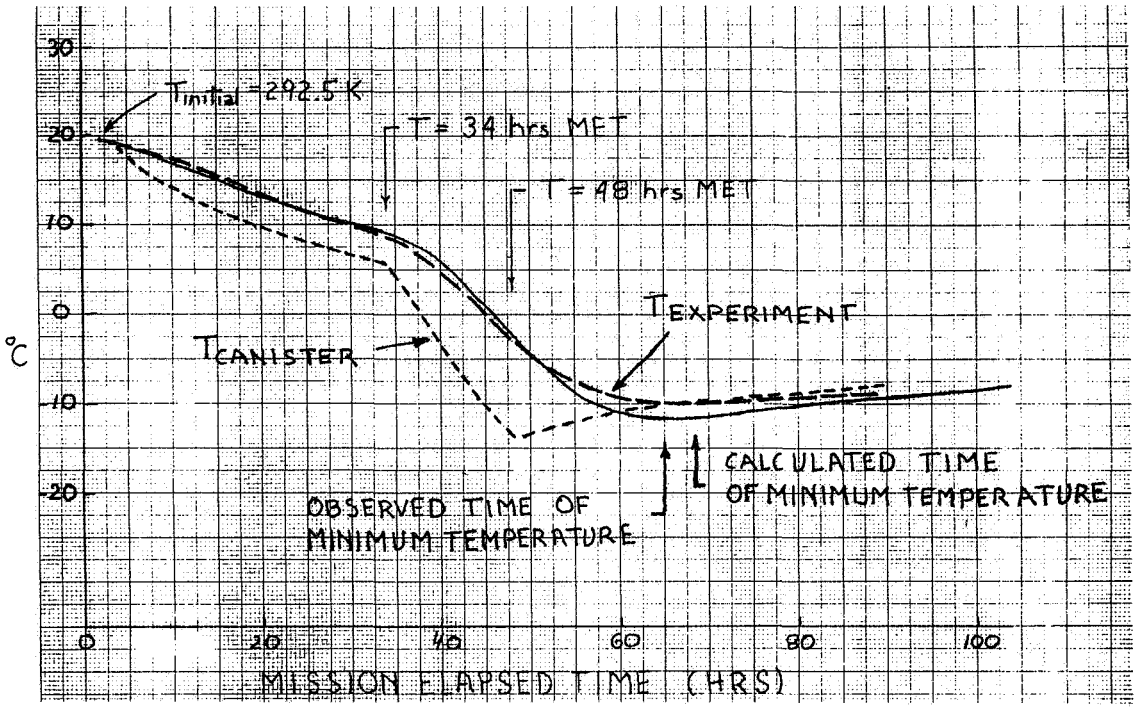

Figure 11. Comparison of G 347 calculated and observed temperatures using reduced experiment thermal conductance and emittance (0.4 of nominal values) and slightly reduced canister emittance (0.055 rather than 0.065).

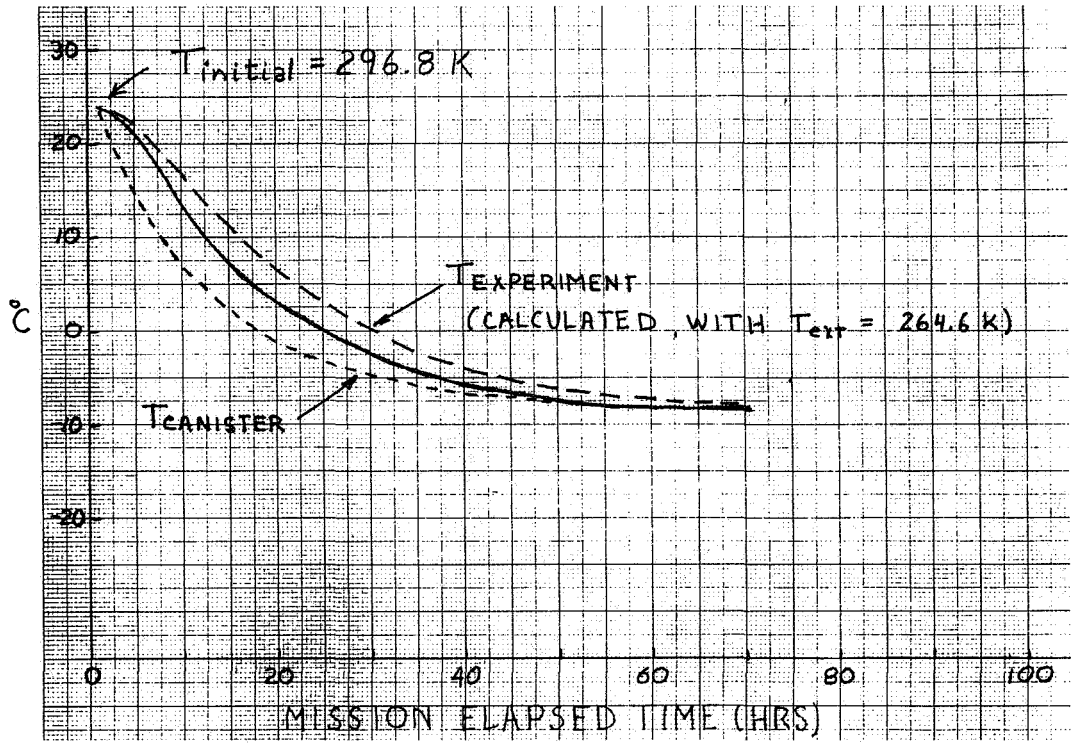

Figure 12. Comparison of G 345 calculated and observed temperatures using reduced experiment thermal conductance and emittance (0.4 of nominal values) and nominal canister emittance (0.16).